Cyclization/Fission and Fragmentation/Recombination Mechanisms for the 1,2 Shift in Free Radicals: A Computational Study of $H_2C^{\bullet}-CH_2X$ (X = −C≡CH, −C≡N, −CH=CH_2, and −CH=NH) and $H_2C^{\bullet}-CH_2CY=O$ (Y = −H, −F, −Cl, $-CH_3$, −CN, −SH, $-SCH_3$, −OH, and $-O^-$)

Philip George,[†] Jenny P. Glusker,*[,†] and Charles W. Bock[†,‡]

The Institute for Cancer Research, Fox Chase Cancer Center, 7701 Burholme Avenue, Philadelphia, Pennsylvania 19111, and Department of Chemistry, Philadelphia University, Henry Avenue and School House Lane, Philadelphia, Pennsylvania 19144

Received: April 6, 2000; In Final Form: August 24, 2000

The role of the cyclopropyl ring structure in the cyclization/fission mechanism for the 1,2 shift of the title radicals, whether as a local minimum on the potential energy surface or as a transition state, has been investigated using density functional theory calculations at the B3LYP/6-31+G*//B3LYP/6-31+G* computational level. The three-membered ring structure, $C_{(1)}-C_{(2)}-C_{(3)}$, has been identified for all the substituent groups, and the alteration in ring geometry that accompanies the changeover in its role has been characterized—notably an increase in the $C_{(1)}-C_{(3)}$ and $C_{(2)}-C_{(3)}$ bond lengths beyond a certain threshold value. The free energy of activation at 298 K for the cyclization/fission mechanism has been compared with that for the alternative fragmentation/recombination mechanism, in which breaking the $C_{(2)}-C_{(3)}$ bond in the initial extended chain structure of the radical, giving an olefin and the radical derived from the substituent group, is followed by $C_{(3)}-C_{(1)}$ bond formation. The difference, $\delta\Delta G^{\ddagger} = \Delta G^{\ddagger}$(frag/recomb) − $\Delta G^{\ddagger}$(cycliz/fiss), whether positive or negative, determines which mechanism is the more likely. With $-C_{(3)}$≡CH, $-C_{(3)}$≡N, and $-C_{(3)}$H=CH_2 as the substituent group, $\delta\Delta G^{\ddagger}$ is positive, indicating that the cyclization/fission mechanism is more favored, whereas with most of the carbonyl substituent groups $\delta\Delta G^{\ddagger}$ is negative, showing the fragmentation/recombination mechanism to be the more favored.

Introduction

The 1,2 shift of unsaturated groups in free radicals provides some striking examples of the influence of structural features on reactivity. Various mechanisms have been put forward to describe this phenomenon; they involve the radicals as such, radical cations, carbanions, and, in the case of the 5′-deoxyadenosylcobalamin-mediated mutase reactions, π-complexes with the Co(II).[1a,b]

Two radical mechanisms in particular for the 1,2 shift date back to the 1960s and -70s.[2a−e] The shift of the vinyl group in the 3-buten-2-methyl-1-yl radical, which gives the 3-buten-2-methyl-2-yl radical, is taken as an example in Chart 1. In the first, a cyclization/fission mechanism, cyclization by the formation of the $C_{(1)}-C_{(3)}$ bond followed by fission of the $C_{(2)}-C_{(3)}$ bond in the ring, brings about the 1,2 shift; see Chart 1A.

In the second, a fragmentation/recombination mechanism, fragmentation by breaking the $C_{(2)}-C_{(3)}$ bond, giving an olefin and the radical derived from the substituent group, followed by recombination, forming the $C_{(3)}-C_{(1)}$, results in the same product, as shown in Chart 1B. If $C_{(1)}$ and $C_{(2)}$ are unsubstituted, or if both carry the same substituent, the 1,2 shift simply regenerates the initial radical. In general, the three-membered ring structure in Chart 1A may be either a higher energy intermediate [a local minimum on the potential energy surface (PES)] or a transition state (TS). The cyclization/fission mechanism is inherently *intramolecular*, whereas the fragmentation/recombination mechanism is *intermolecular* and hence susceptible to confirmation by the formation of crossover products upon admixture with a different olefin.

Ring opening, a feature of the cyclization/fission mechanism, has been extensively studied experimentally in vinyl-substituted radicals,[3a−k] for example, in the 3-buten-1-yl radical itself,[3a,c,f,k] in various methyl derivatives,[3b,d,e,g−k] and in the more complicated radicals

$$Me_2RC\text{-}\dot{C}H_2 \rightarrow Me_2\dot{C}\text{-}CH_2R$$

where R = C_6H_5, $Me_3CC{\equiv}C$, $Me_3CC(=O)$, and N≡C.[4] There was no evidence that would favor the fragmentation/recombination mechanism when R = C_6H_5 or for the migration of C=C double bonds. For those substituents where ring opening has been studied experimentally it is thus reasonable to suppose that, starting with the extended chain structure, the 1,2 shift would occur via the cyclization/fission mechanism.

In the case of the 5′-deoxyadenosylcobalamin-mediated 1,2 shift of the R_1 group;

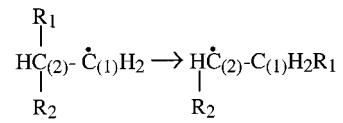

in the α-methyleneglutarate mutase reaction, where R_1 is the substituted vinyl group $-C_{(3)}(COOH){=}CH_2$ and R_2 is −COOH,

* Corresponding author. Tel: 215-728-2220. Fax: 215-728-2863. E-mail: JP_Glusker@fccc.edu.
[†] The Institute for Cancer Research.
[‡] Philadelphia University.

10.1021/jp001318g CCC: $19.00
Published on Web 11/10/2000

CHART 1

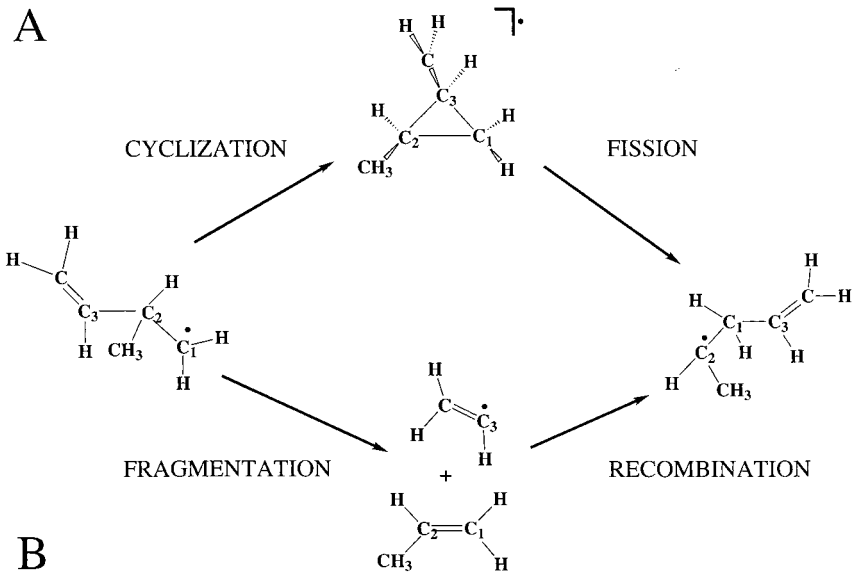

and in the methylmalonate-CoA mutase reaction, where R_1 is the substituted carbonyl group $-C_{(3)}(SCoA)=O$ and R_2 is $-COOH$, some of the experimental results would appear to favor the cyclization mechanism,[5a,b] although stereochemical properties and inhibition experiments provide data favoring the fragmentation/recombination mechanism.[5c−e]

The two mechanisms in Chart 1 represent competing pathways, and the finding that the migration of C=C double bonds in organic systems occurs via the cyclization/fission mechanism (Chart 1A) implies that the free energy of activation is significantly less positive than that for the fragmentation/recombination mechanism (Chart 1B). On the other hand, the difference between these two free energies of activation may well be much smaller for the migration of C=O double bonds—one or the other mechanism being favored depending, for instance, on the substitution pattern and/or environmental factors such as the active site of an enzyme.

To get a better understanding of the structural and electronic features that decide which of these two mechanisms is more likely, we have carried out high-level molecular orbital (MO) calculations for a variety of substituted radicals: (i) radicals of the type $H_2C^{\bullet}-CH_2X$, where X is $-C\equiv CH$, $-C\equiv N$, $-CH=CH_2$, and $-CH=NH$, and (ii) radicals of the type $H_2C^{\bullet}-CH_2-CY=O$, where Y is $-H$, $-F$, $-Cl$, $-CH_3$, $-CN$, $-SH$, $-SCH_3$, $-OH$, and $-O^-$. These substituents have been chosen to determine the effect of changing the number of atoms directly bonded to $C_{(3)}$ from two to three, i.e., changing the connectivity from C2 to C3,[6] and also the effect of substitution by atoms (groups) of different electronegativity.

The three-membered cyclic structure has been identified for all the substituents, and the alteration in ring geometry that accompanies the changeover in its role from a stable intermediate (local minimum on the PES) to a transition state has been characterized. In those cases where the cyclic structure is a stable intermediate, the transition state for its formation has also been identified. Free energies of activation for both the cyclization/fission and the fragmentation/recombination mechanism have been evaluated in each case from the computed values of the ground-state electronic energies at 0 K, the total thermal energies at 298 K, and the entropies at 298 K. The effect of substituting a methyl group on $C_{(2)}$ in 3-buten-1-yl on the formation and properties of the cyclic structure and on the energetics of the fragmentation process have also been investigated.

Computational Methods

The calculations were carried out on computers at the Advanced Scientific Computing Laboratory, NCI-FCRF, using the GAUSSIAN 94 series of programs.[7] Optimizations were performed with density functional theory (DFT) using Becke's three-parameter hybrid method, where the nonlocal correlation functional is that of Lee, Yang, and Parr (B3LYP).[8a−h] The 6-31+G* basis set was employed for all the optimizations. Ground-state electronic energies at 0 K, E_e^0, zero-point energies, zpe; total thermal energies at 298 K, θ; and entropies at 298 K, S^{298}, evaluated from vibrational frequencies, were calculated at the B3LYP/6-31+G*//B3LYP/6-31+G* level, and atomic spin densities were calculated from population analyses using the DFT densities. The vibration frequencies were also used to determine whether the computed structures correspond to local minima (stable intermediates) or to saddle points (transition states) on the potential energy surface, PES.[9a−c] Single-point calculations using second-order Møller−Plesset (MP2) perturbation theory[10a−d] with the more complete 6-311++G(2d,2p) basis set were performed on all the B3LYP/6-31+G*//B3LYP/6-31+G*-optimized structures involved in the cyclization and fragmentation processes. For brevity, the calculations at these two levels will be referred to as "B3LYP" and "MP2" respectively.

These levels are comparable with those employed in recent detailed studies of other radical reactions—notably the prediction of propagation rate coefficients in free radical polymerizations,[11] radical additions to olefins and acetylene,[12a−c] and free radical thermochemistry.[13] Basis set superposition error (BSSE) corrections have not been included because they are very small at the computational levels we have employed,[12c] much smaller than the uncertainties inherent in the computational levels themselves.

No scaling factor was used in the evaluation of the B3LYP/6-31+G* entropies and the thermal energies, it having been found that for a selection of seven small molecules—NH_3, H_2O, $H_2C=CH_2$, $H_2C=O$, $CH_3CH=CH_2$, $CH_3CH=O$, and $HC(=O)-OH$—the calculated values for the entropies are in agreement with experiment, on average, to within 0.17 cal/(mol K) (see Table 1S of the Supporting Information). In the same context, the B3LYP procedure has been shown to perform well in the

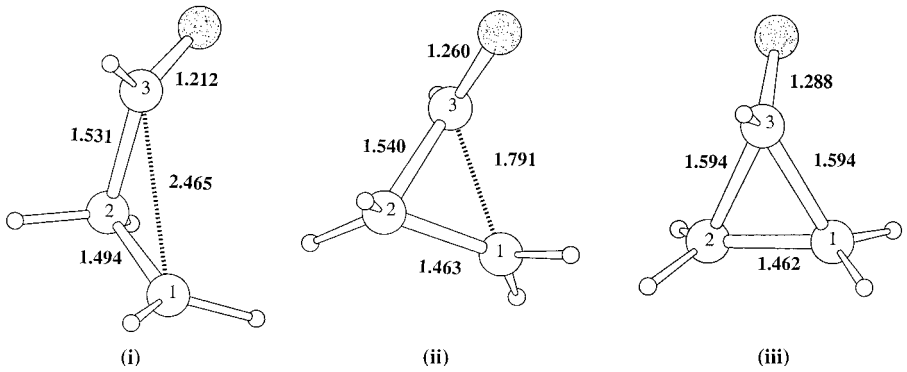

Figure 1. B3LYP-optimized structures of (i) the extended chain, (ii) the contracted chain (TS), and (iii) the symmetrical ring structure of the radical $H_2C^{\bullet}-CH_2-CHO$.

evaluation of zero-point energies[14] and by inference in the further evaluation of total thermal energies.

The sum of E_e^0 and the total thermal energy θ at 298 K gives E^{298}, the total molecular energy at 298 K. Differences in E^{298} values for reactant and product species give the enthalpy changes, ΔH^{298}, which, with the addition of a ΔnRT term where needed, would correspond to experimental gas-phase data.[15] Likewise, differences between the calculated entropy values give the accompanying entropy changes, ΔS^{298}, and hence the free energy changes, using the equation $\Delta G^{298} = \Delta H^{298} - T\Delta S^{298}$. The entropies, zero-point energies, total thermal energies, ground-state electronic energies calculated at the two levels, and the total molecular energies are listed in Table 2S of the Supporting Information. The numbering scheme for the carbon chain used throughout this study is shown in Chart 1.

Results

Radical Structures. The initial radical is found to have an *extended* chain (*trans*) conformation with all the substituents selected for this investigation. The three-membered ring structure is found to be symmetrical, i.e., $C_{(1)}-C_{(3)} = C_{(2)}-C_{(3)}$, and to be a higher energy stable intermediate (local minimum on the PES) for the radicals with $-C\equiv N$, $-CH=CH_2$, $-CF=O$, $-CH=O$, $-CCl=O$, $-C(CH_3)=O$, and $-C(CN)=O$ as the substituent group. The transition state (TS) for the formation of each of these symmetrical ring structures has been identified and found to have a *contracted* chain conformation, i.e., $C_{(1)}$ and $C_{(3)}$ are closer together than in the initial extended chain conformation, but the $C_{(1)}-C_{(3)}$ bond is not fully formed. On the other hand, with $-C(OH)=O$, $-C(SH)=O$, $-C(SCH_3)=O$, and $-C(O)-O^-$ as the substituent group, the symmetrical ring structure is the transition state for the 1,2 shift, rather than being a local minimum on the PES.

The B3LYP/6-31+G*-optimized internuclear distances $C_{(1)}-C_{(2)}$, $C_{(1)}-C_{(3)}$, and $C_{(2)}-C_{(3)}$ in the extended chain, the contracted chain (TS), and the ring structure (local minimum or TS) for each substituent group are listed in Table 3S in rank order of increasing $C_{(1)}-C_{(3)}$ ($C_{(2)}-C_{(3)}$) bond distance in the ring structure. Typical structures are depicted in Figure 1 for the formyl derivative ($C_{(1)}^{\bullet}H_2-C_{(2)}H_2-C_{(3)}H=O$). The contraction of the chain structure in forming the transition state for the formation of the stable ring structure is shown very clearly by the decrease in the nonbonded distance $C_{(1)}\cdots C_{(3)}$, on average from 2.48 ± 0.02 to 1.81 ± 0.09 Å. Taking the change in this distance as the criterion, the extent of ring closure in the transition state is rather less for the substituents $-CH=CH_2$, its $C_{(2)}-Me$ derivative, *cis*- and *trans*-$CH=NH$, and $-C\equiv N$, than for $-CH=O$, $-C(CH_3)=O$, $-CF=O$, $-CCl=O$, and $-C(CN)=O$, on average 66% compared to 83%. A notable feature of these data is the changeover in the role of the symmetrical ring structure from local minimum on the PES to transition state for the 1,2 shift as the $C_{(1)}-C_{(3)}$ and $C_{(2)}-C_{(3)}$ bond distances exceed 1.606 Å.

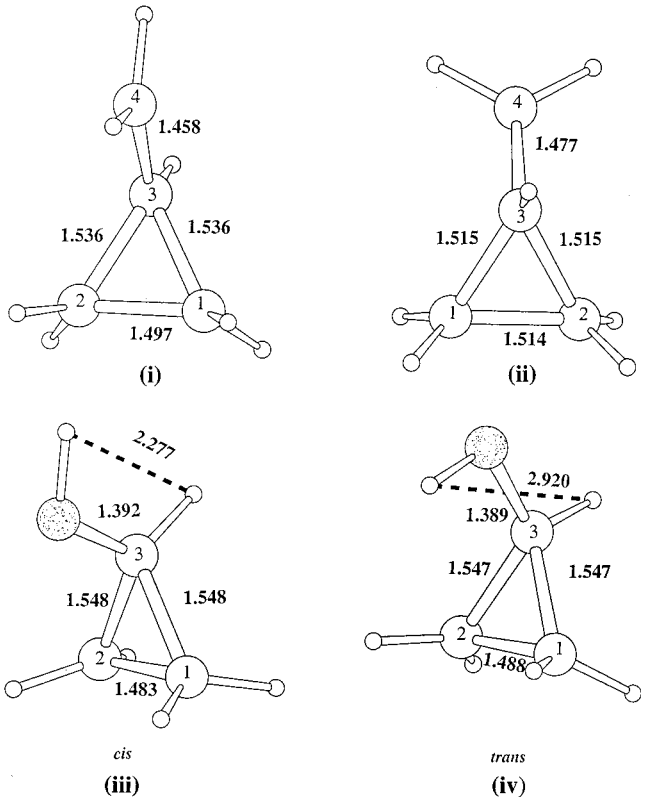

Figure 2. B3LYP-optimized structures of (i) the symmetrical ring structure of the radical $H_2C_{(1)}-C_{(2)}H_2-C_{(3)}H=CH_2$ and (ii) the transition state for the rotation of the $-CH_2$ group about the $C_{(3)}-C$ bond axis in this radical. (iii and iv) The cis and trans geometrical isomers, respectively, of the symmetrical ring structures of the radical $H_2C^{\bullet}-CH_2-CH=NH$.

With the vinyl group as substituent ($C_{(1)}^{\bullet}H_2-C_{(2)}H_2-C_{(3)}H=CH_2$) two conformers of the ring structure have been identified, in accord with calculations reported in the literature[14,16−18] (see Figure 2, parts i and ii). In the lower energy conformer (i) (a local minimum on the PES) the two H-atoms of the exocyclic H_2C- group lie in a plane that bisects the ring plane, as suggested by ESR studies).[16,19] In the higher energy conformer (ii) (a TS on the PES, which can be assigned as the TS for rotation of the H_2C- group about the $C-C_{(3)}$ bond axis), one of the H-atoms of the H_2C- group now eclipses the proximal H-atom bonded to $C_{(1)}$, while the other eclipses the proximal H-atom bonded to $C_{(2)}$. The energy barrier, $\Delta H^{\ddagger}$, is found to be

CHART 2

2.5_7 and 2.5_3 kcal/mol at the B3LYP and MP2 levels, respectively. The value of $\Delta S^{\ddagger}$ is quite small but negative, -2.7 cal/(mol K), in keeping with the changes in $C_{(1)}-C_{(2)}$, $C_{(2)}-C_{(3)}$, and $C_{(1)}-C_{(3)}$ bond lengths, and gives values for $\Delta G^{\ddagger}$ of 3.4 and 3.3 kcal/mol. Using the rate equation

$$k = \frac{\kappa kT}{h} e^{-\Delta G^{\ddagger}/RT}$$

assuming the transmission coefficient κ to be unity, the rate constants are 2.0 and 3.4×10^{10} s^{-1} and the corresponding half-reaction time is $\approx 3 \times 10^{-11}$ s, showing the rotation to be an extremely rapid process. Compared with the experimental Arrhenius activation energy of 2.7 kcal/mol, measured over the range 125−155 K,[16] the predicted values at a mean temperature of 140 K are in very close agreement, 2.9 and 2.8 kcal/mol at the two levels, respectively. Previous calculations reported in the literature[14] have given 3.5 kcal/mol (CBS−RAD), 3.0 kcal/mol (B3LYP/6-31G(d)), 3.4 kcal/mol (B3LYP/6-311+G(d,p)), and 3.5 kcal/mol (B3LYP/6-311+G(3df,2p)).

With the formimino group $-CH_C{=}NH_N$ as substituent there are *cis* and *trans* geometrical isomers; see Chart 2. The shorter $H_C\cdots H_N$ internuclear distance in the cis isomers of the extended chain, the contracted chain, and the ring structure is, on average, 2.26 ± 0.02 Å compared to the longer internuclear distance in the trans isomers, which, on average, is 2.90 ± 0.02 Å. The cis and trans isomers of the symmetrical ring structure are depicted in Figure 2iii and iv. In the cis isomer H_N is 3.54 Å from the proximal H-atoms on $C_{(1)}$ and $C_{(2)}$ and 4.04 Å from the distal H-atoms, whereas in the trans isomer these distances are significantly less, 2.49 and 3.65 Å, respectively. These shorter distances in the trans isomer, notably that between H_N and the proximal H-atoms, are accompanied by an appreciable relaxation of the carbon−carbon bonding in the ring compared to that in the cis isomer. $C_{(1)}-C_{(3)}$ and $C_{(2)}-C_{(3)}$ are longer by 0.026 Å and $C_{(1)}-C_{(2)}$ by 0.005 Å; see Table 3S. The cis isomers of the extended chain, the contracted chain, and the ring structure are consistently lower in energy than the corresponding trans isomers by 0.8, 1.3, and 0.9 kcal/mol and 1.0, 1.4, and 0.6 kcal/mol at the B3LYP and MP2 levels, respectively. In the fragmentation radicals $C_{(3)}{\bullet}H-NH$, the stability relationship is reversed. The trans isomer is lower in energy than the cis isomer by 5.0 and 4.5 kcal/mol, respectively, at these two levels.

The substituent group $-C{\equiv}CH$ provides an interesting exception to the dual role for the symmetrical ring structure as either a local minimum on the PES or as a transition state; see the first entry in Table 3S. In this case, although the contracted chain structure (Figure 3ii) is again a transition state, it leads to the formation of an *unsymmetrical* ring structure (Figure 3iii), as a local minimum on the PES. *The symmetrical* ring structure (Figure 3iv) is a transition state for the interconversion of the two equivalent forms of the unsymmetrical structure in which the H-atom bonded to the exocyclic C-atom is situated nearer to $C_{(2)}$, as in Figure 3iii, or nearer to $C_{(1)}$. The enthalpy of activation, $\Delta H^{\ddagger}$, for this interconversion is found to be 2.9 and 2.1 kcal/mol at the B3LYP and MP2 levels, respectively. $\Delta S^{\ddagger}$ is nearly zero, -0.16 cal/(mol K), so $\Delta G^{\ddagger} \approx \Delta H^{\ddagger}$. Assuming a transmission coefficient of unity, these values give 4.6×10^{10} and 1.8×10^{11} s^{-1} for the rate constant, with half-reaction times

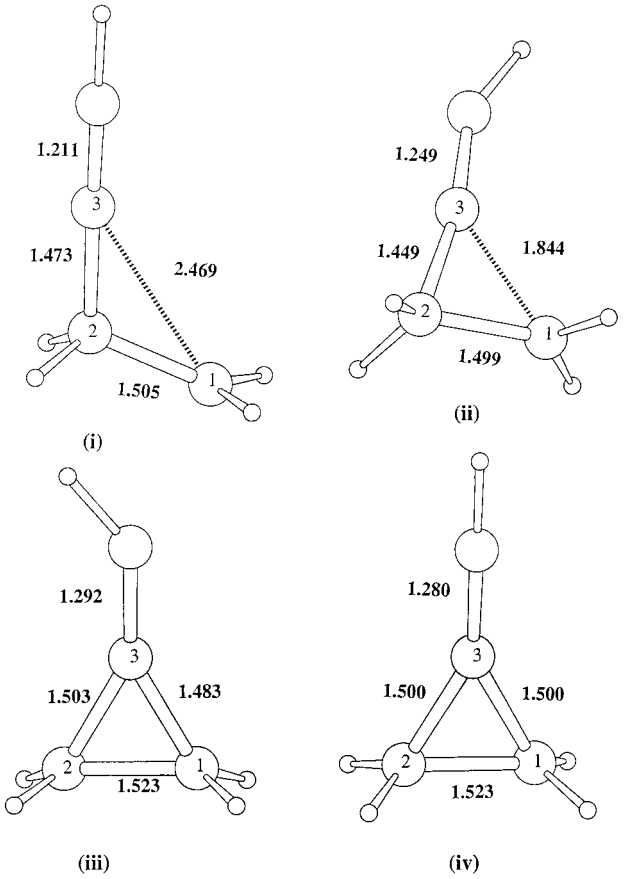

Figure 3. B3LYP -optimized structures of (i) the extended chain, (ii) the contracted chain (TS), and (iii) the unsymmetrical ring structure (loc. min. on the PES) of the radical $H_2C_{(1)}{\bullet}-C_{(2)}H_2-C_{(3)}{\equiv}CH$. (iv) The symmetrical ring structure of the radical, i.e., the transition state for the libration in the $C-C_{(3)}-C_{(2)}-C_{(1)}$ plane of the H-atom bonded to the C-atom of the CH group in the unsymmetrical ring structure from the side nearer to $C_{(2)}$ to the side nearer to $C_{(1)}$.

from about 10^{-11} to 10^{-12} s. Since the interconversion amounts to a wagging motion of a H-atom, tunneling would result in an increase in the transmission coefficient, and hence, the rate constant has to be considered. The increase has been estimated using Wigner's transmission coefficient, $\kappa^{w}(T)$, given by the expression

$$\kappa^{w}(T) = 1 + \frac{1}{24}\left(\frac{\hbar\omega^{\ddagger}}{RT}\right)^2$$

where $\omega^{\ddagger}$ is the imaginary frequency of the unbound normal mode at the saddle point.[20] From the vibration frequency analysis $\omega^{\ddagger}$ is found to have a value a little less than 700 cm^{-1}, which, upon substitution in the above expression, gives $\kappa^{w}(298) = 1.5$. The interconversion would thus proceed about 1.5 times faster with the correction than without.

The bond lengths in the substituent groups are listed in Table 4S. There is a progressive increase in the length of the bond between $C_{(3)}$ and the multiple-bonded exo heavy atom (C, O, or N) as one goes from the extended chain, to the contracted chain, to the symmetrical (local minimum) ring structure. In the other cases where the symmetrical ring structure is the transition state, there is a comparable increase in going from the extended chain to the ring structure, except in the case of the negatively charged carboxylate group.

Atomic Spin Densities. The changes in structure in going from the extended to the contracted chain and then to the ring structure are reflected in the redistribution of atomic spin density.

The listing in Table 5S shows that it is localized on $C_{(1)}$ in all the extended chain structures, as would be expected; see Figures 1i and 3i. As the ring begins to form in the contracted chain structure, the density is divided between $C_{(1)}$ and the multiple-bonded exo heavy atom. In the symmetrical ring structures, both those that are local minima on the PES and those that are transition states, the spin density is mainly on the exo heavy atom, although in most cases there is also a significant density on $C_{(1)}$ and $C_{(2)}$. This is particularly noticeable in the case of the negatively charged carboxylate group, where the equivalence of the two charge-bearing O-atoms evidently prevents any buildup of spin density in that part of the structure.

Charge Separation, Valence Orbital Populations, and Natural Bond Orbitals in the Ring Structures. These properties have been studied to see if there is any correlation with the role of the ring structure as a local minimum on the PES or as the transition state for the 1,2 shift. Values for the atomic charges on the component atoms and the valence orbital populations have been obtained from natural population analyses (NPA)[21] using the B3LYP densities and are listed in Tables 6S and 7S and in Table 8S, respectively, of the Supporting Information.

To characterize the charge separation, three structural elements have been selected: (i) $C_{(3)}$, the apical carbon atom in the three-membered ring; (ii) the side-chain, i.e., the exocyclic atoms of the substituent group moiety; and (iii) the carbon and hydrogen atoms of the ring in toto, $H_2C_{(2)}C_{(3)}C_{(1)}H_2$. The charges on these three elements, q.$C_{(3)}$, q.exo, and q.ring are listed in columns i, ii, and iii of Table 9S. With $-C_{(3)}\equiv CH$ and $-C_{(3)}H=CH_2$ as the substituent group, there is charge transfer from the substituent moiety to the ring, q.exo is positive, and q.ring is negative; whereas with an electronegative atom in the substituent group moiety, the transfer is in the opposite direction. The values of q.$C_{(3)}$ are primarily responsible for the trend shown by the values of q.ring. Taking all the values in Table 7S into account, with the exception of these for the carboxylate derivative, the range for the H-atoms is 0.25−0.27, with a mean of 0.26 ± 0.01, and the range for $C_{(1)}$ and $C_{(2)}$ is 0.41−0.48, with a mean of 0.44 ± 0.02. The effect of electronegative atom bonding in the substituent group moiety is shown very clearly by the charge on $C_{(3)}$. With $-C_{(3)}\equiv CH$ as the substituent group, replacement of CH by N in the $-C_{(3)}-CH$ moiety results in a change in q.$C_{(3)}$ from −0.17 to 0.12: with $-C_{(3)}H-CH_2$ as the substituent group, replacement of CH_2 in the $-C_{(3)}H-CH_2$ moiety, first by NH, then by O, results in a progressive change from −0.35 to −0.14 and then to 0.11, in accord with the increasing electronegativity.[22] Replacement of the H-atom in $-C_{(3)}H-O$ by an additional electronegative atom leads to even more positive values: e.g., F, 0.67; C1, 0.29; OH, 0.00, etc.

Hydrogen is the least electronegative atom in these structures,[22] and the charge separation is primarily the result of a decrease in electron occupancy in the 1s orbital of the hydrogen and a corresponding increase in the occupancy in the valence orbitals of C, N, O, F (S and Cl). In most cases the occupancy in these 2p(3p) orbitals exceeds the nominal values of 4, 5, 6, and 7, respectively, for the unbound atoms; see Table 8S. The only exceptions are the 2p occupancy values for carbon triply bonded to nitrogen or doubly bonded to oxygen in the various carbonyl derivatives. With the change in the connectivity of carbon from 2 to 3 to 4, as exemplified by the values for $C_{(3)}$ and C with $-C_{(3)}\equiv CH$ and $-C_{(3)}H=CH_2$ as the substituent group, there is only a slight increase in the 2p orbital occupancy. To sum up, despite well-defined differences in the values of q.$C_{(3)}$, q.exo, q.ring, and the valence orbital populations, there is no indication of threshold values that would mark the changeover in the role of the ring structure from local minimum to transition state on the PES. A close examination of the natural bond orbitals has likewise found no criteria for distinguishing between these two roles.

TABLE 1: Enthalpy, Entropy, and Free Energy Changes at 298 K, in kcal/mol, cal/(mol K), and kcal/mol, Respectively, for the Formation of the Stable Ring Structure (Local Minimum on the PES) from the Extended Chain Structure, Calculated at the B3LYP Level (Upper Values) and at the MP2 Level (Lower Values)

substituent group	ΔH^{298}	ΔS^{298}	ΔG^{298}
$-C_{(3)}H=CH_2$[a]	3.0	−3.2	4.0
	2.3	−3.2	3.3
$-C_{(3)}H=CH_2$	3.4	−3.9	4.5
	2.3	−3.9	3.5
cis $-C_{(3)}H=NH$	6.2	−6.3	8.1
	9.0	−6.3	10.9
trans $-C_{(3)}H=NH$	6.3	−6.1	8.1
	8.6	−6.1	10.4
$-C_{(3)}(CN)=O$	7.7	−5.9	9.5
	14.0	−5.9	15.8
$-C_{(3)}\equiv CH$[b]	8.2	−5.5	9.8
	14.8	−5.5	16.4
$-C_{(3)}H=O$	9.2	−5.6	10.9
	16.3	−5.6	18.0
$-C_{(3)}(CH_3)=O$	12.3	−6.7	14.3
	18.2	−6.7	20.2
$-C_{(3)}Cl=O$	15.4	−5.5	17.0
	23.4	−5.5	25.0
$-C_{(3)}F=O$	17.1	−5.5	18.8
	25.7	−5.5	27.4
$-C_{(3)}\equiv N$	16.8	−5.4	18.4
	27.6	−5.4	29.2

[a] Methyl group substitution on $C_{(2)}$. [b] Unsymmetrical ring structure; see Figure 3(iii).

The Fragmentation Radicals. The bond lengths in the radical species derived from the substituent groups, produced by fission of the $C_{(2)}-C_{(3)}$ bond in the extended chain structures, are listed in Table 4S. The bond lengths between $C_{(3)}$ and the adjacent multiple-bonded heavy atom fall into two categories. In the first, in which $C_{(3)}$ in the substituent group has connectivity C2, i.e., $-C_{(3)}\equiv CH$ and $-C_{(3)}\equiv N$, the bond length is longer in the fragmentation radical than in the extended chain structure. In the second, in which $C_{(3)}$ has connectivity C3 and which includes all the other substituent groups, it is shorter. With $-C_{(3)}\equiv CH$ and $-C_{(3)}H=CH_2$, in which $C_{(3)}$ is triply and doubly bonded to carbon, the atomic spin density in the fragmentation radical is almost exclusively on $C_{(3)}$; see Table 5S. For all the other substituent groups, however, in which $C_{(3)}$ is multiple-bonded to one or more electronegative atoms, the spin density tends to be delocalized, with significant density on N, O, Cl, and S.

Thermodynamic Data for Ring Closure. Values of ΔH^{298}, ΔS^{298}, and ΔG^{298} for the formation of the ring by closure of the extended chain structure are listed in Table 1 in rank order of increasingly positive values of ΔH^{298}. ΔS^{298} is consistently negative, as would be expected for ring closure, but small in magnitude, ranging from −3.2 to −6.7 cal/(mol K), with the result that ΔG^{298} is slightly more positive than ΔH^{298}.

With the exception of $-CH=CH_2$ and the $C_{(2)}$-methyl derivative, ΔH^{298} for the remaining substituent groups is significantly larger at the MP2 level than at the B3LYP level, although the same rank order is followed and with it the trend in ΔG^{298} to quite large positive values. This type of discrepancy has been observed in the case of a simpler reaction by Dobbs and Dixon.[23] We note, however, that at the B3LYP level the rotation of the exocyclic CH_2 group in the vinyl ring structure

TABLE 2: Energy Values at 0 K in kcal/mol, for (i) Extended Chain Structure → Contracted Chain Structure (TS), (ii) Extended Chain Structure → Ring Structure (local minimum on PES), and (iii) Ring Structure (local minimum on PES) → Contracted Chain Structure (TS), i.e. the Ring Opening Reaction, Calculated from the Molecular Energies, E_e^0 + zpe, Using the Values of E_e^0 and zpe at the B3LYP Level Listed in Table 2S

substituent group	$\Delta H^{\ddagger}$ (i)	ΔH (ii)	$\Delta H^{\ddagger}$ (iii)
−CH═CH_2[a]	10.0	3.3	6.7
−CH═CH_2	10.8	3.8	7.0
cis-CH═NH	10.8	6.8	4.0
trans-CH═NH	11.2	7.0	4.2
−C≡CH	15.7	9.0	6.7
−C≡N	20.1	17.5	2.6
−C(CN)═O	8.7	8.3	0.4
−CH═O	10.1	9.8	0.3
−C(CH_3)═O	12.9	12.9	0.0
−CCl═O	15.7	15.9	−0.2
−CF═O	17.4	17.6	−0.2

[a] Methyl group substitution on $C_{(2)}$.

is accounted for satisfactorily. In themselves these ΔH^{298}, ΔS^{298}, and ΔG^{298} values could be an indication that, for the 1,2 shift to occur, the fragmentation/recombination mechanism is preferable.

The Potential Energy Surface in the Region of the Ring Structure. As can be seen from a comparison of the values of ΔH(ii) and $\Delta H^{\ddagger}$(i) in Table 2, with −CH═CH_2, its $C_{(2)}$-methyl derivative, and −C≡CH as substituent groups, and to a lesser extent −C≡N, the ring structures (local minima on the PES's) are lower in energy than the transition states for their formation — the contracted chain structures. The difference, $\Delta H^{\ddagger}$(i) − ΔH(ii) is the energy barrier, $\Delta H^{\ddagger}$(iii), for the ring opening step. These ring structures are thus distinct reaction intermediates at the B3LYP level, although undergoing rapid fission to give the extended chain structure. On the other hand, with the carbonyl group substituents, −C(CN)═O through −CF═O in Table 2, $\Delta H^{\ddagger}$(i) and ΔH(ii) are nearly the same. For these substituent groups the potential energy surface is evidently almost flat in this region. In the case of the other carbonyl group substituents, −C(OH)═O, −C(SH)═O, −C(SCH_3)═O, and −C(O^-)═O (see Table 3S), no contracted chain structure could be identified as a transition state, and in its place, the ring structure takes over as the transition state for the 1,2 shift. As far as reactivity is concerned, there is no operational difference between these two classes of carbonyl-substituted radicals. In both cases generation of the cyclic radical would result in ring opening to give the extended chain structure without activation.

Enthalpies, Entropies, and Free Energies of Activation for the 1,2 Shift via Cyclization/Fission and via Fragmentation/Recombination. The activation process for the fragmentation/recombination mechanism has been taken to be the splitting of the extended chain structure into a smaller radical species and a vinyl structure; see Chart 1B. The presence of an actual transition state would clearly result in a slower reaction. For example, in the case of −CH═O, −CCl═O, and −C(OH)═O as substituents, transition states have been located at the MP2 level, 6.3, 2.7, and 4.8 kcal/mol in energy above the combined energies of the fragmentation species, giving rate constants 10^{-3}−10^{-4} times slower.

With this proviso in mind, the results of these calculations are given in Table 3 for both mechanisms in rank order of less positive (more negative) values of $\delta\Delta G^{\ddagger}$, where

$$\delta\Delta G^{\ddagger} = \Delta G^{\ddagger}(\text{frag/recomb}) - \Delta G^{\ddagger}(\text{cycliz/fiss})$$

TABLE 3: Enthalpies, Entropies, and Free Energies of Activation at 298 K, in kcal/mol, cal/(mol K), and kcal/mol, Respectively, for the 1,2 Shift in the Radical $RC_{(2)}H_2-C_{(1)}{}^{\bullet}H_2$ via the Cyclization/Fission Mechanism and via the Fragmentation/Recombination Mechanism, Calculated at the B3LYP Level (upper values) and at the MP2 Level (lower values)

substituent group, R	cyclization/fission $\Delta H^{\ddagger}$	$\Delta S^{\ddagger}$	$\Delta G^{\ddagger}$	fragmentation/recombination $\Delta H^{\ddagger}$	$\Delta S^{\ddagger}$	$\Delta G^{\ddagger}$	$\delta\Delta G^{\ddagger}$[d]
−C≡CH[a]	15.0	−4.9	16.5	58.1	31.6	48.7	32.2
	18.2	−4.9	19.7	60.7	31.6	51.3	31.6
−C≡N[a]	19.4	−5.5	21.0	56.1	28.9	47.5	26.5
	26.0	−5.5	27.6	63.1	28.9	54.5	26.9
−CH═CH_2[a]	10.1	−5.7	11.8	32.6	34.3	22.4	10.6
	9.0	−5.7	10.7	36.4	34.3	26.2	15.5
−CH═CH_2[a,b]	9.3	−5.6	11.0	29.4	38.6	17.9	6.9
	8.0	−5.6	9.7	35.2	38.6	23.7	14.0
cis-CH═NH[a]	9.9	−7.1	12.0	26.1	33.1	16.3	4.3
	10.8	−7.1	12.9	29.7	33.1	19.9	7.0
trans-CH═NH[a]	10.4	−6.3	12.3	20.3	33.5	10.3	−2.0
	11.0	−6.3	12.9	24.2	33.5	14.2	1.3
−CF═O[a]	16.5	−7.7	18.8	28.3	33.8	18.2	−0.6
	23.8	−7.7	26.1	30.2	33.8	20.1	−6.0
−CH═O[a]	9.2	−6.4	11.1	17.2	33.2	7.3	−3.8
	12.8	−6.4	14.7	16.4	33.2	6.5	−8.2
−CCl═O[a]	14.9	−7.0	17.0	18.6	35.1	8.1	−8.9
	20.7	−7.0	22.8	21.2	35.1	10.7	−12.1
−C(CH_3)═O[a]	12.1	−7.7	14.4	14.7	35.3	4.2	−10.2
	14.9	−7.7	17.2	17.7	35.3	7.2	−10.0
−C(CN)═O[a]	7.9	−6.6	9.9	18.3	34.9	7.9	−2.0
	11.6	−6.6	13.6	27.9	34.9	17.5	3.9
−C(OH)═O[c]	20.9	−7.3	23.1	24.1	33.8	14.0	−9.1
	26.8	−7.3	29.0	26.6	33.8	16.5	−12.5
−C(SH)═O[c]	17.2	−6.6	19.2	13.0	34.7	2.7	−16.5
	24.0	−6.6	26.0	15.8	34.7	5.5	−20.5
−C(SCH_3)═O[c]	17.8	−9.9	20.8	14.7	34.2	4.5	−16.3
	24.5	−9.9	27.5	19.2	34.2	9.0	−18.5
−C(O^-)═O[c]	27.1	−5.0	28.6	8.8	33.4	−1.1	−29.7
	24.9	−5.0	26.4	11.9	33.4	2.0	−24.4

[a] Transition state: contracted chain structure. [b] Methyl group substitution on $C_{(2)}$. [c] Transition state: ring structure. [d] $\delta\Delta G^{\ddagger}$ gives the difference between the two free energies of activation, i.e. $\delta\Delta G^{\ddagger}$ = $\Delta G^{\ddagger}$(fragmentation/recombination) − $\Delta G^{\ddagger}$(cyclization/fission).

This difference shows directly which mechanism is more likely: if positive, cyclization/fission, if negative, fragmentation/recombination. There is clearly a very abrupt changeover in the shift mechanism. With −C≡CH, −C≡N, −CH═CH_2, and the $C_{(2)}$-methyl derivative, cyclization/fission is definitely favored, in accord with the substantial body of experimental evidence.[3a−j,4] On the other hand, there is a clear preference for the fragmentation/recombination mechanism with most of the carbonyl substituent groups, although −CF═O and −CH═O could be borderline cases.

A particularly striking example of the interplay between the thermodynamic parameters that determine which mechanism is operative is provided by the data with −C≡N as the substituent. Although ΔG^{298} for the formation of the ring structure has an especially large positive value — which alone would point to fragmentation/recombination — $\Delta G^{\ddagger}$ for its formation is not much larger. However, $\Delta G^{\ddagger}$ for fragmentation/recombination is far larger still, so much so that the outcome is clearly in favor of cyclization/fission.

Comparison of Calculated Values of $\Delta H^{\ddagger}$ and ΔH for Cyclopropylcarbinyl Radical Reactions with Experimental Values and with Other Calculated Values in the Literature. High-level calculations of $\Delta H^{\ddagger}$ for the ring opening of the cyclopropylcarbinyl radical and ΔH for the formation of the extended chain 3-buten-1-yl radical have recently been

TABLE 4: Comparison of Calculated and Experimental Values for the Energy Barrier, $\Delta H^{\ddagger}$, and the Enthalpy Change, ΔH, for Ring Opening of the Cyclopropylcarbinyl Radical[a]

computational level	ref	$\Delta H^{\ddagger}$	ΔH
PMP2/6-31G*//HF/6-31G*	3k[b]	7.6_4	-4.8_2
QCISD/6-31G*//HF/6-31G*	3k[b]	9.7_1	-3.8_8
G2	3k[b]	8.3_3	-3.7_8
CBS-RAD[c]/QCISD//HF/6-31G(d)	14	7.8_9	-2.2_5
CBS-RAD[c]/B3LYP//HF/6-31G(d)	14	7.8_6	-2.1_7
B3LYP/6-31G(d)//B3LYP/6-31G(d)	14	8.6_7	-2.2_7
B3LYP/6-311G(3df,2p)//B3LYP/6-31G(d)	14	7.3_4	-3.3_7
B3LYP/6-31+G(d)//B3LYP/6-31+G(d)	this work	7.7_2	-2.9_6
MP2(FULL)/6-311++G(2d,2p)//B3LYP/6-31+G(d)	this work	7.6_5	-1.9_5
experiment[d]		7.4_6	-1.6_5, -1.9_1, -2.7_7, -4.6_4

[a] Values in kcal/mol at 0 K without zero-point energy contributions. [b] Values at 298 K corrected to 0 K without zero-point and thermal energy contributions, using the values of θ obtained in this work. [c] See ref e in ref 14. [d] References for these experimental values, in this order, are given in the footnotes to Table 1 in ref 14.

reported.[3k,14] Typical values, without the inclusion of zero-point energy contributions, along with those obtained experimentally likewise adjusted to 0 K, are listed in Table 4. The values obtained in the present study at the B3LYP and the MP2 levels (lines 4 and 5) compare very favorably both with experiment and the other high-level computational values. The predicted values for the rate constant for ring opening at 298 K are 5.6 and 6.4 $\times$ 10^7 s^{-1}, respectively, in close agreement with the experimental value of 9.6 $\times$ 10^7 s^{-1} and the CBS−RAD value of 4.9 $\times$ 10^7 s^{-1}.[14] The values obtained for the barrier to rotation of the H_2C- group about the $C-C_{(3)}$ bond axis are also very close to other computation results (see above), and the agreement with the experimental Arrhenius activation energy at 140 K[17] is, on average, to within 0.1 kcal/mol.

Methyl group substitution on $C_{(2)}$ is found to give a slightly lower barrier for ring opening (see Table 2), in accord with other high-level calculations.[3k] The far slower migration aptitude with $N{\equiv}C-$ as substituent is borne out by the experimental results for the $C_{(2)}$-dimethyl structure, but direct comparison for acetylenic and formyl substituents cannot be made because the structures were far more extensively substituted, i.e., $-C{\equiv}CCMe_3$ and $-C(CMe_3){=}O$.[4] The data in Table 1 are compatible with the comparable rates found experimentally for the $C_{(2)}$-dimethyl derivatives with $-CH{=}CH_2$ and $-CH{=}O$ as substituents, although the calculated values for the barrier heights using 3-21G-optimized structures are appreciably greater, 14.9 and 19.2 kcal/mol, respectively.[24]

There have been far fewer computational studies of the fragmentation/recombination mechanism. A revealing comparison was made for several substituent groups using the MNDO SCF-MO procedure with the unrestricted Hartree−Fock (UHF) option for the open shell species and optimization of all geometrical variables.[25] But the MNDO method is known to predict too high an activation energy for simple 1,2-hydrogen migrations,[26] so the values obtained for the activation energies in this MNDO study are probably also too high.[25]

Summary and Conclusions

The calculations reported above have shown that the two most important structural features which determine whether the 1,2 shift in free radicals of the type $H_2C^{\bullet}-CH_2X$ would occur preferentially via the cyclization/fission mechanism or via the fragmentation/recombination mechanism are the connectivity of the apical carbon atom in the three-membered ring, $C_{(3)}$, and the bonding of an electronegative atom or atoms to $C_{(3)}$.

With the hydrocarbon substituent groups $-C_{(3)}{\equiv}CH$ and $-C_{(3)}H{=}CH_2$, $C_{(3)}$ in the ring structures has connectivity C3 and C4, respectively; see Figure 3 and Chart 1. $\delta\Delta G^{\ddagger}$, the difference between the free energies of activation for the fragmentation/recombination and the cyclization/fission mechanism, is large and positive in each case (see Table 6), a clear indication that a 1,2 shift via the cyclization/fission mechanism is the more likely. With CH in $-C_{(3)}{\equiv}CH$ replaced by the electronegative N-atom, $\delta\Delta G^{\ddagger}$ is reduced in value, but still quite positive, whereas with an O-atom replacing H_2C in $H_2C{=}C_{(3)}H-$ to give the formyl group (see Figure 1), $\delta\Delta G^{\ddagger}$ is negative, indicating that fragmentation/recombination has become the more favored mechanism.

In considering the more likely mechanism for the α-methyleneglutarate and the methylmalonate-CoA mutase reactions, an additional factor has to be taken into account. There is a diminution in the translational entropies of species reacting in the restricted spatial environment at the active site of the enzyme due to the far smaller molal volumes.[27] As a consequence, $\Delta G^{\ddagger}$ for fragmentation in which there are two product species in relation to the one reactant species would be more positive by about 4.7 kcal/mol, and in turn, $\delta\Delta G^{\ddagger}$ would be more positive (less negative) to the same extent.[25] The present results are strong presumptive evidence for a cyclization mechanism in the case of α-methyleneglutarate mutase, where $C_{(3)}$ is the carbon atom of a vinyl group, since the $\delta\Delta G^{\ddagger}$ values for the 3-buten-1-yl radical and its 2-methyl derivative are large and positive and would only be augmented by the translational entropy correction. In the case of methylmalonate-CoA mutase, where $C_{(3)}$ is the carbon atom of a carbonyl group, even though $\delta\Delta G^{\ddagger}$ has rather low negative values for some carbonyl substituent groups, with $HS-C(=O)-$, and $CH_3S-C(=O)-$, the $\delta\Delta G^{\ddagger}$ values exceed −16 kcal/mol, so that with allowance made for the translational entropy correction the values would still be large and negative, and hence strongly in favor of the fragmentation/recombination mechanism. In other mutase reactions such as glutamate mutase and ornithine mutase, where $C_{(3)}$ is bonded to a carbon atom whose connectivity is C4, ring formation is not possible and the 1,2 shift is limited either to fragmentation/recombination or to some kind of concerted mechanism.

Acknowledgment. We thank the Advanced Scientific Computing Laboratory, NCI-FCRF, for providing time on the CRAY YMP supercomputer. The authors would also like to acknowledge the technical support provided by Carol Afshar and the comments of a reviewer that made a significant contribution to the manuscript. This work was supported by Grants CA-10925 and CA-06927 from the National Institutes of Health and by an appropriation from the Commonwealth of Pennsylvania. Its contents are solely the responsibility of the authors and do not necessarily represent the official views of the National Cancer Institute.

Supporting Information Available: Tables of data as noted in the text. This material is available free of charge via the Internet at http://pubs.acs.org.

References and Notes

(1) (a)Halpern, J. *Science* **1985**, *277*, 869−875. (b)Wollowitz, S.; Halpern, J. *J. Am. Chem. Soc.* **1988**, *110*, 3112−3120.

(2) (a)Slaugh, L. H.; Mullineaux, R. D.; Raley, J. H. *J. Am. Chem. Soc.* **1963**, *85*, 3180−3183. (b)Urry, W. H.; Trecker, D. J.; Hartzler, H. D. *J. Org. Chem.* **1964**, *29*, 1663−1669. (c)Montgomery, L. K.; Matt, J. W.; Webster, J. R. *J. Am. Chem. Soc.* **1967**, *89*, 923−934. (d)Montgomery, L. K.; Matt, J. W. *J. Am. Chem. Soc.* **1967**, *89*, 6556−6564. (e)Bertini, F.; Caronna, T.; Grossi, L.; Minisci, F. *Gazz. Chim. Ital.* **1974**, *104*, 471−478.

(3) (a)Maillard, B.; Forrest, D.; Ingold, K. U. *J. Am. Chem. Soc.* **1976**, *98*, 7024−7026. (b)Castaing, M.; Pereyre, M.; Ratier, M.; Blum, P. M.; Davies, A. G. *J. Chem. Soc., Perkin II* **1979**, 287−292. (c)Effio, A.; Griller, D.; Ingold, K. U.; Beckwith, A. L. J.; Serelis, A. K. *J. Am. Chem. Soc.* **1980**, *102*, 1734−1736. (d) Ingold, K. U.; Warkentin, J. *Can. J. Chem.* **1980**, *58*, 348−352. (e) Chatgilialoglu, C.; Ingold, K. U.; Tse-Sheepy, I.; Warkentin, J. *Can. J. Chem.* **1983**, *61*, 1077−1081. (f) Newcomb, M.; Glenn, A. G. *J. Am. Chem. Soc.* **1989**, *111*, 275−277. (g) Newcomb, M.; Glenn, A. G., Williams, W. G. *J. Org. Chem.* **1989**, *54*, 2675−2681. (h) Beckwith, A. L. J.; Bowry, V. W. *J. Org. Chem.* **1989**, *54*, 2681−2688. (i) Bowry, V. W.; Lusztyk, J.; Ingold, K. U. *J. Am. Chem. Soc.* **1991**, *113*, 5687−5698. (j) Nonhebel, D. C.; Suckling, C. J.; Walton, J. C. *Tetrahedron Lett.* **1982**, *23*, 4477−4480. (k)Martinez, F. N.; Schlegel, H. B.; Newcomb, M. *J. Org. Chem.* **1996**, *61*, 8547−8550.

(4) Lindsay, D. A.; Lusztyk, J.; Ingold, K. U. *J. Am. Chem. Soc.* **1984**, *106*, 7087−7093; see p 7089.

(5) (a) Ashwell, S.; Davies, A. G.; Golding, B. T.; Hay-Motherwell, R.; Mwesigye-Kibende, S. *J. Chem. Soc. Chem. Commun.* **1989**, 1483−1485. (b) Scott, A. I.; Karuso, P.; Williams, H. J.; Lally, J.; Robinson, J.; Nayar, G. P. *J. Am. Chem. Soc.* **1994**, *116*, 777−778. (c) Beatrix, B.; Zelder, O.; Kroll, F. K.; Örlygsson, G.; Golding, B. T.; Buckel, W. *Angew. Chem., Int. Ed. Engl.* **1995**, *34*, 2398−2403. (d) Edwards, C. H.; Golding, B. T.; Kroll, F.; Beatrix, B.; Bröker, G.; Buckel, W. *J. Am. Chem. Soc.* **1996**, *118*, 4192−4193. (e)Buckel, W.; Golding, B. T. *Chem. Soc. Rev.* **1996**, 329−337.

(6) Pople, J. A.; Gordon, M. *J. Am. Chem. Soc.* **1967**, *89*, 4253−4261.

(7) Frisch, M. J.; Trucks, G. W.; Schlegel, H. B.; Gill, P. M. W.; Johnson, B. G.; Robb, M. A.; Cheeseman, J. R.; Keith, T.; Petersson, G. A.; Montgomery, J. A.; Raghavachari, K.; Al-Laham, M. A.; Zakrzewski, V. G.; Ortiz, J. V.; Foreman, J. B.; Cioslowski, J.; Stefanov, B. B.; Nanayakkara, A.; Challacombe, M.; Peng, C. Y.; Ayala, P. Y.; Chen, W.; Wong, M. W.; Andres, J. L.; Repogle, E. S.; Gomperts, R.; Martin, R. L.; Fox, D. J.; Binkley, J. S.; Defrees, D. J.; Baker, J.; Stewart, J. P.; Head-Gordon, M.; Gonzalez, C.; Pople, J. A. *Gaussian 94, Revision E.2*: Gaussian Inc., Pittsburgh, PA, 1995.

(8) (a) Becke, A. D. *Phys. Rev.* **1988**, *A38*, 3098−3100. (b) Becke, A. D. *J. Chem. Phys.* **1993**, *98*, 1372−1377. (c) Becke, A. D. *J. Chem. Phys.* **1993**, *98*, 5648−5652. (d) Lee, C.; Yang, W.; Parr, R. G. *Phys. Rev.* **1988**, *B37*, 785−789. (e) Vosko, S. H.; Wilk, L.; Nusair, M. *Can. J. Phys.* **1980**, *58*, 1200−1211. (f) Perdew, J. P.; Wang, Y. *Phys. Rev. B* **1992**, *45*, 13244−13249. (g) Perdew, J. P. In *Electronic Structure of Solids;* Ziesche, P., Eischrig, H., Eds.; Akademie Verlag: Berlin, 1991. (h) Perdew, J. P.; Chevary, J. A.; Vosko, S. H.; Jackson, K. A.; Pederson, M. R.; Singh, D. J.; Fiolhais, C. *Phys. Rev. B* **1992**, *46*, 6671−6687.

(9) (a) McIver, J. W., Jr.; Kormornicki, A. *J. Am. Chem. Soc.* **1972**, *94*, 2625−2633. (b) Pople, J. A.; Krishnan, R.; Schlegel, H. B.; Binkley, J. S. *Int. J. Quantum Chem. Symp.* **1979**, *13*, 225−241. (c) Schlegel, H. B. In *New Theoretical Concepts for Understanding Organic Reactions;* Bertran, J., Csizmadia, I. G., Eds.; Kluwer: Academic Publishers: Dordrecht, The Netherlands, 1989; pp 33−53.

(10) (a) Hariharan, P. C.; Pople, J. A. *Theor. Chim. Acta* **1973**, *28*, 213−222. (b) Binkley, J. S.; Pople, J. A. *Int. J. Quantum Chem.* **1975**, *9*, 229−236. (c) Møller, C.; Plesset, M. S. *Phys. Rev.* **1934**, *46*, 618−622. (d) Pople, J. A.; Binkley, J. S.; Seeger, R. *Int. J. Quantum Chem. Symp.* **1976**, *10*, 1−19.

(11) Heuts, J. P. A.; Gilbert, R. G.; Radom, L. *Macromolecules* **1995**, *28*, 8771−8781.

(12) (a) Wong, M. W.; Radom, L. *J. Phys. Chem.* **1995**, *99*, 8582−8588. (b) Wong, M. W.; Radom, L. *J. Phys. Chem. A* **1998**, *102*, 2237−2245. (c) Barone, V.; Orlandini, L. *Chem. Phys. Lett.* **1995**, *246*, 45−52.

(13) Mayer, P. M.; Parkinson, C. J.; Smith, D. M.; Radom, L. *J. Chem. Phys.* **1998**, *108*, 604−615.

(14) Smith, D. M.; Nicolaides, A.; Golding, B. T.; Radom, L. *J. Am. Chem. Soc.* **1998**, *120*, 10223−10233 and references therein.

(15) Del Bene, J. E. In *Molecular Structure and Energetics;* Liebman, J. F., Greenberg, A., Eds.; VCH Publishers: Deerfield Beach, FL, 1986; Vol. 1, Chapter 9.

(16) Walton, J. C. *Magn. Reson. Chem.* **1987**, *25*, 998−1000.

(17) Hehre, W. J. *J. Am. Chem. Soc.* **1973**, *95*, 2643−2646.

(18) Quenemoen, K.; Borden, W. T.; Davidson, E. R.; Feller, D. *J. Am. Chem. Soc.* **1985**, *107*, 5054−5059.

(19) Kochi, J. K.; Krusic, P. J.; Eaton, D. R. *J. Am. Chem. Soc.* **1969**, *91*, 1877−1879.

(20) Garrett, B. C.; Truhlar, D. G. *J. Am. Chem. Soc.* **1979**, *83*, 200−203.

(21) Reed, A. E.; Weinstock, R. B.; Weinhold, F. *J. Chem. Phys.* **1985**, *83*, 735−746.

(22) Allen, L. C. *J. Am. Chem. Soc.* **1989**, *111*, 9003−9014, and references therein.

(23) Dobbs, K. D.; Dixon, D. A. *J. Phys. Chem.* **1994**, *98*, 12584−12589.

(24) Giese, B.; Heinrich, N.; Horler, H.; Koch, W.; Schwarz, H. *Chem. Ber.* **1986**, *119*, 3528−3535.

(25) Russell, J. J.; Rzepa, H. S.; Widdowson, D. A. *J. Chem. Soc. Chem. Commun.* **1983**, 625−627.

(26) Kyba, E. P. *J. Am. Chem. Soc.* **1977**, *99*, 8330−8332.

(27) George, P.; Siegbahn, Per E. M.; Glusker, J. P.; Bock, C. W. *J. Phys. Chem. B* **1999**, *103*, 7531−7541.